

## Induced transparency and absorption in coupled whispering-gallery microresonators

Ahmer Naweed, G. Farca, S. I. Shopova, and A. T. Rosenberger\*

*Department of Physics, Oklahoma State University, Stillwater, Oklahoma 74078-3072, USA*

(Received 19 November 2004; published 5 April 2005)

Optical behavior analogous to electromagnetically induced transparency and absorption is observed in experiments using coupled fused-silica microspheres. This behavior results from interference between coresonant whispering-gallery modes of the two spheres. Coupled-resonator-induced transparency and absorption are observed. Which effect is seen depends on the strength of coupling of incident light from a tapered fiber into the first sphere and on the strength of coupling between the two spheres. The observed effects can enhance microresonator performance in various applications.

DOI: 10.1103/PhysRevA.71.043804

PACS number(s): 42.60.Da, 42.50.Gy, 42.81.Wg

Like electrons in a Bohr atom, light in submillimeter dielectric spheres circulates in ringlike orbits. Such “photonic atoms” [1] are actually optical microresonators, and the “orbits” are the so-called whispering-gallery modes (WGMs). The extraordinary properties of these WGMs [2] enable various microresonator-based applications such as cavity quantum electrodynamics (CQED) [3], microlasers [4–6], biosensing [7], and trace-gas and analyte detection [8,9]. WGMs are conveniently and efficiently excited by tunneling of photons from an adjacent tapered optical fiber into the microresonator. Typical WGMs propagate along the sphere’s equator and their evanescent field component allows interaction with the surrounding environment. By bringing two spheres nearly into contact, their WGMs can be evanescently coupled. Recent theoretical analysis of coupled microresonators has revealed that coherence effects in the coupled-resonator system are remarkably similar to those in atoms [10]. Here we demonstrate experimental observation of induced transparency and absorption in coupled microspheres due to interference between their respective coresonant WGMs. These are classical analogs of electromagnetically induced transparency (EIT) [11] and absorption (EIA) [12–14], quantum interference effects that reduce or enhance light absorption in a coherently driven atom.

The key concept underlying electromagnetically induced transparency and absorption is coherence among certain atomic states, achieved by coupling these states using coherent light sources. In one case, absorption from the ground state to a nearly degenerate pair of coherent superposition states can vanish due to destructive interference between the transition probability amplitudes. Such a medium, therefore, exhibits a narrow transparency window within its usual absorption profile. In contrast, EIA is characterized by constructive interference, resulting in enhanced absorption at line center. As solid-state alternatives to atomic ensembles, crystalline materials [15] and semiconductor heterostructures [16] have also been studied. All such systems, however, rely on quantum interference to diminish or enhance absorption. As examples of classical systems, models demonstrating EIT in plasmas have been investigated theoretically [17] and lin-

early coupled *RLC* circuits have been shown to exhibit EIT-like features [18]. In addition, recent theoretical works have examined various optical-resonator configurations for observing classical analogs of EIT [10,19,20]. Here we use spherical microresonators and experimentally achieve coupled-resonator-induced transparency (CRIT) and absorption (CRIA) purely on the basis of classical optical interference between WGMs. We also demonstrate that coupling between the two microresonators can result in linewidth narrowing and amplitude enhancement of certain modes.

Fiber coupling of incident laser light into a microsphere is analogous to the use of a partially transmitting mirror in a model ring cavity whose other mirrors have zero transmission. In the model, part of the incident light is transmitted through the mirror and coupled into the resonator, while the uncoupled light is reflected off. In a fused-silica microresonator, because of the intrinsic loss (predominantly scattering) each whispering-gallery resonance appears as a Lorentzian dip in the coupling fiber throughput. The fractional dip depth  $M$  of a whispering gallery resonance can be expressed in terms of the loss ratio  $x=T/al$  as  $M=4x/(1+x)^2$ , while the dip width is proportional to the total round-trip loss  $T+al$ . Here,  $T$  is the effective mirror transmittance describing the fiber coupling loss, and the microresonator intrinsic round-trip loss is given by  $al$ , where  $\alpha$  is the effective loss coefficient and  $l$  the microresonator circumference. The dip depth reaches its maximum value  $M=1$  at critical coupling ( $x=1$ ). The dip depth depends upon the amplitudes of the light coming out of the sphere and the initially uncoupled light; since their phase difference is  $\pi$ , they interfere destructively. For critical coupling, the two amplitudes are equal. The net throughput (reflectivity in the model) on resonance is  $R=1-M$ .

Coupling a second microsphere to the first (but not directly to the fiber) alters the observed WGM spectrum, depending on how close the second sphere is to being coresonant with the first and on the strength of the coupling between spheres. By controlling the sphere separation  $d$ , the intersphere coupling can be varied. Figure 1(a) shows a simplified view of light trajectories inside coupled microresonators, modeled as coupled ring cavities; a schematic of the experimental system is shown in the inset of Fig. 1(b). Consider first the case where the two spheres are resonant at the

\*Electronic address: atr@okstate.edu

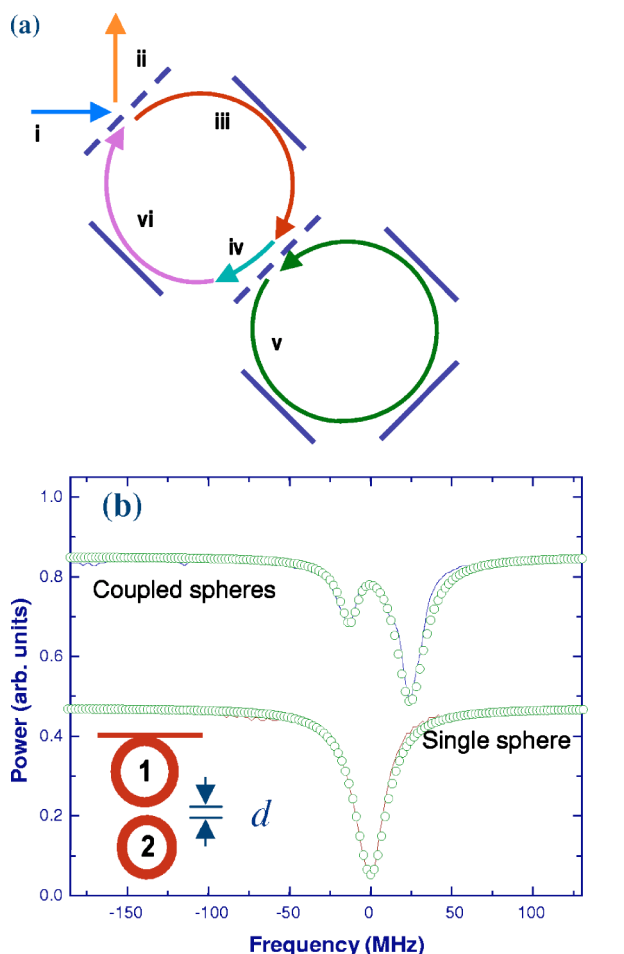


FIG. 1. (Color online) (a) Schematic of the coupled-ring-cavity model. Partially transmitting mirrors (dashed lines) represent coupling between the fiber and the first sphere and coupling between the two microspheres. The incident light (i) is partially reflected (ii), and partially coupled into the first sphere (iii). On encountering the second sphere, part of this light is reflected (iv) and continues its propagation inside the first sphere, while part of the light is transmitted into the second sphere (v). Light from the second sphere tunnels back into the first sphere and interferes with the light circulating there. Part of the resulting wave (vi) escapes and interferes destructively with the initially reflected signal (ii). (b) Mode splitting in noncoresonant coupled microspheres with radii  $a_1=240$  and  $a_2=200 \mu\text{m}$ . The two traces have the same scale, but different vertical axis origins. The single-sphere dip has  $M=0.69$ . Solid curves, experimental data; circles, calculated profiles based on coupled-ring-cavity model. Inset: a schematic of the experimental configuration.

same frequency. The effective intrinsic loss of the first sphere's WGM increases with intersphere coupling as the effective reflectivity of the second cavity decreases from unity. Coupling between spheres is relatively weak when they are not in contact, so the second sphere has a higher  $Q$  and narrower resonance than the first. If the original mode is undercoupled ( $x < 1$ ), adding the second sphere drives the system farther from critical coupling over the second sphere's resonance width. The result is a decrease in dip depth at the center of the resonance of the first sphere; this

narrow peak appearing in the middle of the original dip is a manifestation of CRIT. If the original mode is overcoupled ( $x > 1$ ), addition of loss from the second sphere will initially drive the system toward critical coupling, producing a sharp drop at the middle of the original dip, i.e., CRIA. When the two spheres are not coresonant, new dips can appear in the spectrum as the intersphere coupling increases. These belong to strongly undercoupled modes of the second sphere or, in some instances, strongly overcoupled modes of the first sphere.

The CRIT-EIT analogy is discussed in detail in Ref. [10], where it is shown, for example, that the inter-resonator coupling is analogous to the strength of the coupling (or pump) field in EIT. Because the first resonator is undercoupled, the net throughput (reflection) is out of phase with the out-coupled intracavity field. The dip in the former is the signal of loss in the first resonator, and a decrease in the latter is the signal of loss in the second resonator. Hence they interfere destructively to give CRIT. When the first resonator is overcoupled, the net throughput and outcoupled field are in phase, and constructive interference gives CRIA. This is analogous to the transfer of coherence in certain degenerate two-level systems that results in constructive interference in absorption and thus EIA [12–14]. With increasing pump field and ac Stark splitting, EIA turns into EIT [13], though the transparency window is not quite as narrow in frequency as the enhanced absorption [14]. Precisely the same behavior is observed in the coupled-resonator model as the inter-resonator coupling increases.

In this work the microspheres were fabricated by melting the tip of a fused-silica fiber in a hydrogen-oxygen flame. Due to surface tension, the molten silica turns into a nearly perfect sphere with smooth surface finish. However, minor spheroidal deformation lifts the symmetry degeneracy and results in a rich WGM spectrum. An adiabatically tapered single-mode fiber ( $3.4 \mu\text{m}$  diameter) was used to couple the incident laser light into the first microsphere. The fiber was tangent to the microsphere in its equatorial plane; the setup was very similar to that described earlier [6]. A tunable diode laser ( $\lambda=1540\text{--}1570 \text{ nm}$ ) and microspheres with intrinsic quality factors ( $Q$ ) in the range of  $10^6\text{--}10^8$  were used. The sphere diameters were measured to within about  $\pm 5 \mu\text{m}$  with an optical microscope. Using a precision actuator, the separation between the second (outer) sphere and the first sphere could be varied. It is neither necessary to make microspheres identical in size, nor to tune one sphere, to obtain coresonance. Instead, because of the high density of WGM spectra, it is possible to find coincident resonances in the two microspheres simply by tuning the laser wavelength. For coresonant modes symmetric mode splitting occurs [21,22]; for noncoincident WGMs, however, asymmetric features are seen, as in Fig. 1(b). The fit to the ring-cavity model shown in Fig. 1(b) uses the intersphere coupling, the intrinsic  $Q$  of the second sphere, and the frequency offset of the WGMs as fitting parameters. This will be described in detail elsewhere. Here and in subsequent figures the modes of the coupled microspheres are aligned with those of the single resonator at the origin of the relative frequency axis for clarity, although there may be a frequency shift due to change in the WGM effective index of refraction on varying the intersphere coupling.

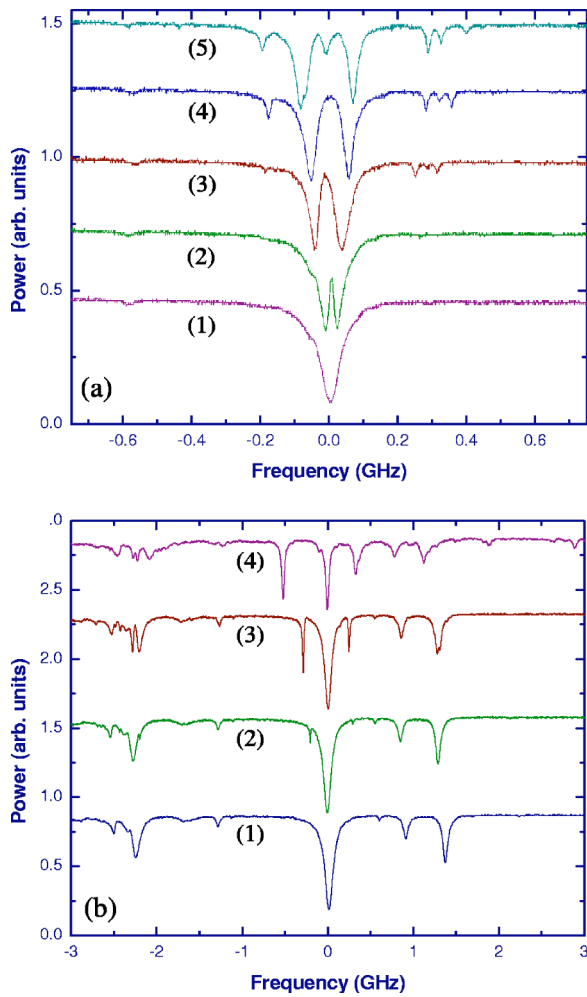


FIG. 2. (Color online) (a) Induced transparency in coupled coresonant microspheres with radii  $a_1=240$  and  $a_2=375$   $\mu\text{m}$ . The traces have the same scale, but different vertical shifts. The dip in trace 1 has  $M=0.43$ . (b) Linewidth narrowing in the same coupled microspheres as in (a), but without coresonance. The traces have the same scale, but different vertical shifts. The central dip in trace 1 has  $M=0.67$ . In both (a) and (b), the coupling between microspheres increases with increasing trace number, the decrease in sphere separation  $d$  for successive traces is of the order of  $1$   $\mu\text{m}$ , and trace 1 is for the first microresonator alone.

Figure 2(a) shows induced transparency in the whispering gallery spectrum of two coupled microspheres with coresonant WGMs. The first sphere is undercoupled, and the second sphere has a  $Q$  that is nearly an order of magnitude greater than that of the first. At weak intersphere coupling, a narrow peak appears in the middle of the throughput dip due to destructive interference between the modes. This transparency spike grows in strength with increased coupling (larger trace number) and the original mode eventually splits into two [23]. In this limit, the coherence of the interaction is still evident in the fact that each of the two split modes has about half the width of the original. The weak dip within the transmission peak of trace 5 in Fig. 2(a) probably represents the appearance of a mode of the second sphere with orthogonal polarization and thus decoupled. The input polarization was

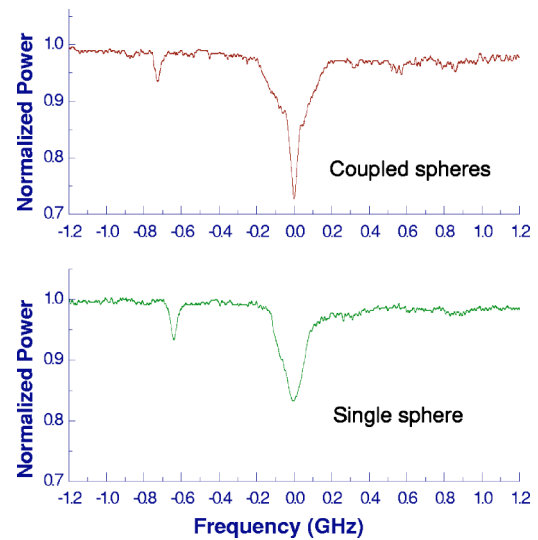


FIG. 3. (Color online) Induced absorption in coupled microresonators with radii  $a_1=180$  and  $a_2=220$   $\mu\text{m}$ .

not controlled, so both TE (transverse electric) and TM (transverse magnetic) WGMs could be excited. Figure 2(b) shows the effect of intersphere coupling on WGM linewidth for three noncoincident coupled modes, the central one in the first sphere and the two satellites in the second sphere. On increasing the coupling (increasing trace number), the modes of the second sphere appear in the spectrum, grow in amplitude, and shift away from the center. As this happens, the linewidth of the original mode decreases, approaching one-third of its original width, and the two satellites broaden to the same width as the narrowed central mode. This happens because, as the intersphere coupling increases, so does the frequency range over which modes can coherently interact, and for sufficiently high  $Q$  of the second sphere the mode widths will approach the original width divided by the number of interacting modes [24]. The observation of induced absorption is displayed in Fig. 3, where an initially overcoupled WGM of the first sphere, upon interaction with a coresonant WGM of the second sphere, is driven toward critical coupling.

Numerical calculations (to be detailed elsewhere) indicate that under conditions of large mode splitting, the frequency shift of the split modes in coupled microspheres can exhibit a strong sensitivity to the effective intrinsic loss of the second resonator. This effect can play a critical role in sensing applications not just as a means of enhancing the WGM evanescent-wave absorption sensor, but rather as an alternative to amplitude-variation-based sensing. Additionally, the linewidth narrowing has the potential to improve microresonator performance in nonlinear optics, microlasers, and CQED experiments.

To conclude, our experimental results show that interference between coresonant WGMs in coupled microspheres results in classical analogs of EIT and EIA with potential applications as noted above. In addition, the dispersive features of coupled microresonators [10], such as slow light velocities, are also analogous to those of a coherently driven

atomic medium, making coupled resonators an ideal tool to explore these effects of optical coherence.

This work was supported by the Oklahoma Center for the Advancement of Science and Technology under Project No.

AR022-052 and by the National Science Foundation under Awards No. ECS-0115442 and No. ECS-0329924. The authors thank M. J. Humphrey, E. Dale, D. K. Bandy, and D. D. Smith for valuable discussions.

- 
- [1] S. Arnold, *Am. Sci.* **89**, 414 (2001).
- [2] V. B. Braginsky, M. L. Gorodetsky, and V. S. Ilchenko, *Phys. Lett. A* **137**, 393 (1989).
- [3] D. W. Vernooy, A. Furusawa, N. P. Georgiades, V. S. Ilchenko, and H. J. Kimble, *Phys. Rev. A* **57**, R2293 (1998).
- [4] V. Sandoghdar, F. Treussart, J. Hare, V. Lefèvre-Seguin, J.-M. Raimond, and S. Haroche, *Phys. Rev. A* **54**, R1777 (1996).
- [5] S. M. Spillane, T. J. Kippenberg, and K. J. Vahala, *Nature (London)* **415**, 621 (2002).
- [6] S. I. Shopova, G. Farca, A. T. Rosenberger, W. M. S. Wickramanayake, and N. A. Kotov, *Appl. Phys. Lett.* **85**, 6101 (2004).
- [7] S. Arnold, M. Khoshshima, I. Teraoka, S. Holler, and F. Vollmer, *Opt. Lett.* **28**, 272 (2003).
- [8] A. T. Rosenberger and J. P. Rezac, in *Biomedical Instrumentation Based on Micro- and Nanotechnology*, edited by R. P. Mariella, Jr. and D. V. Nicolau, Proceedings of the SPIE Vol. 4265 (SPIE, Bellingham, WA, 2001), p. 102.
- [9] E. Krioukov, D. J. W. Klunder, A. Driessen, J. Greve, and C. Otto, *Opt. Lett.* **27**, 1504 (2002).
- [10] D. D. Smith, H. Chang, K. A. Fuller, A. T. Rosenberger, and R. W. Boyd, *Phys. Rev. A* **69**, 063804 (2004).
- [11] K.-J. Boller, A. Imamoglu, and S. E. Harris, *Phys. Rev. Lett.* **66**, 2593 (1991).
- [12] A. M. Akulshin, S. Barreiro, and A. Lezama, *Phys. Rev. A* **57**, 2996 (1998).
- [13] A. Lezama, S. Barreiro, and A. M. Akulshin, *Phys. Rev. A* **59**, 4732 (1999).
- [14] A. Lezama, S. Barreiro, A. Lipsich, and A. M. Akulshin, *Phys. Rev. A* **61**, 013801 (1999).
- [15] Y. Zhao, C. Wu, B.-S. Ham, M. K. Kim, and E. Awad, *Phys. Rev. Lett.* **79**, 641 (1997).
- [16] H. Schmidt, K. L. Campman, A. C. Gossard, and A. Imamoglu, *Appl. Phys. Lett.* **70**, 3455 (1997).
- [17] G. Shvets and J. S. Wurtele, *Phys. Rev. Lett.* **89**, 115003 (2002).
- [18] C. L. Garrido Alzar, M. A. G. Martinez, and P. Nussenzveig, *Am. J. Phys.* **70**, 37 (2002).
- [19] T. Opatrný and D.-G. Welsch, *Phys. Rev. A* **64**, 023805 (2001).
- [20] L. Maleki, A. B. Matsko, A. A. Savchenkov, and V. S. Ilchenko, *Opt. Lett.* **29**, 626 (2004).
- [21] V. S. Ilchenko, M. L. Gorodetsky, and S. P. Vyatchanin, *Opt. Commun.* **107**, 41 (1994).
- [22] T. Mukaiyama, K. Takeda, H. Miyazaki, Y. Jimba, and M. Kuwata-Gonokami, *Phys. Rev. Lett.* **82**, 4623 (1999).
- [23] Mode splitting may also occur due to internal backscattering that couples a high- $Q$  WGM to the counterpropagating mode, but this does not give rise to sharp spectral features. See D. S. Weiss *et al.*, *Opt. Lett.* **20**, 1835 (1995).
- [24] D. D. Smith, H. Chang, and K. A. Fuller, *J. Opt. Soc. Am. B* **20**, 1967 (2003).